OMP Peptides Activate the DegS Stress-Sensor Protease by a Relief of Inhibition Mechanism

Citation: Sohn, Jungsan, Robert A. Grant, and Robert T. Sauer. "OMP Peptides Activate the DegS Stress-Sensor Protease by a Relief of Inhibition Mechanism." Structure 17, no. 10 (October 2009): 1411–1421. © 2009 Elsevier Ltd.

As Published: http://dx.doi.org/10.1016/j.str.2009.07.017

Publisher: Elsevier B.V.

Persistent URL: http://hdl.handle.net/1721.1/96266

Version: Final published version: final published article, as it appeared in a journal, conference proceedings, or other formally published context

Structure
Article

OMP Peptides Activate the DegS Stress-Sensor Protease by a Relief of Inhibition Mechanism

Jungsan Sohn,[1] Robert A. Grant,[1] and Robert T. Sauer[1,*]
[1]Department of Biology, Massachusetts Institute of Technology, Cambridge, MA 02139, USA
*Correspondence: bobsauer@mit.edu
DOI 10.1016/j.str.2009.07.017

SUMMARY

In the *E. coli* periplasm, C-terminal peptides of misfolded outer-membrane porins (OMPs) bind to the PDZ domains of the trimeric DegS protease, triggering cleavage of a transmembrane regulator and transcriptional activation of stress genes. We show that an active-site DegS mutation partially bypasses the requirement for peptide activation and acts synergistically with mutations that disrupt contacts between the protease and PDZ domains. Biochemical results support an allosteric model, in which these mutations, active-site modification, and peptide/substrate binding act in concert to stabilize proteolytically active DegS. Cocrystal structures of DegS in complex with different OMP peptides reveal activation of the protease domain with varied conformations of the PDZ domain and without specific contacts from the bound OMP peptide. Taken together, these results indicate that the binding of OMP peptides activates proteolysis principally by relieving inhibitory contacts between the PDZ domain and the protease domain of DegS.

INTRODUCTION

Intracellular proteases are ubiquitous in biology, where they function in regulatory pathways and in protein quality control. Because of the intrinsically destructive nature of these enzymes, their activities are usually highly regulated (Hauske et al., 2008). For example, degradation by proteases in the HtrA family is controlled by ligand-induced changes in enzyme conformation (Kim and Kim, 2005). These multimeric molecular machines, which function as trimers or higher oligomers, are widely conserved and implicated in pathogenesis in bacteria and many diseases in humans (Ehrmann and Clausen, 2004; Vande Walle et al., 2008). Each HtrA subunit contains a trypsin-like protease domain and one or two regulatory PDZ domains. How the activities of HtrA proteases are allosterically regulated is an important question, which is just beginning to be understood for a few family members.

Escherichia coli DegS is an HtrA-family protease that catalyzes the rate-limiting activation step in the σ^E envelope-stress response (for reviews, see Alba and Gross, 2004; Kim and Kim, 2005; Ades, 2008). Each DegS subunit contains one serine-protease domain and one PDZ domain. The functional protease is a trimer, which is anchored to the periplasmic side of the inner membrane via N-terminal sequences. Under normal conditions of cell growth, the proteolytic activity of DegS is minimal. However, when heat shock or other environmental stresses disrupt protein folding in the periplasm, DegS is activated to cleave RseA, a membrane-spanning protein whose cytoplasmic domain binds and inhibits σ^E (Ades et al., 1999; Alba et al., 2002; Grigorova et al., 2004). This initial site-1 cleavage primes intramembrane site-2 proteolysis of RseA by RseP (Alba et al., 2002). After site-2 cleavage, the complex of σ^E with the cytoplasmic domain of RseA is released from the inner-membrane, and the remaining portions of RseA in this complex are subsequently degraded by cytoplasmic ATP-dependent proteases (Flynn et al., 2004; Chaba et al., 2007). The liberated σ^E then binds RNA polymerase and activates transcription of specific stress-response genes (Rhodius et al., 2006).

How is DegS activity regulated? Peptides ending with Tyr-Xxx-Phe (YxF) bind to the DegS PDZ domain and dramatically increase proteolytic cleavage of the RseA substrate in vitro (Walsh et al., 2003). This C-terminal sequence motif is present in many outer-membrane porins (OMPs), including those whose overexpression activates DegS in vivo. Moreover, the YxF motif is inaccessible in membrane-imbedded OMPs (Baslé et al., 2006), suggesting that misfolded OMPs in the periplasm activate DegS, thereby initiating the envelope-stress response. Crystal structures of DegS, with and without bound OMP peptides, show that the peptide-binding site is almost 20 Å from the enzyme active site, which is malformed in the peptide-free enzyme (Wilken et al., 2004; Zeth, 2004). Thus, peptide activation is allosteric. Biochemical experiments also indicate that saturation of the enzyme with the RseA substrate and with OMP peptides is necessary for maximal activation of DegS (Figure 1A; Sohn and Sauer, 2009).

Two mechanisms have been proposed to explain how OMP peptides activate DegS. The inhibition-relief model postulates a dynamic equilibrium between inactive and active DegS conformations, with peptide binding driving the equilibrium toward the active state by disrupting inhibitory interactions mediated by the PDZ domain (Walsh et al., 2003; Sohn et al., 2007; Sohn and Sauer, 2009). In the peptide-activation model, by contrast, specific contacts between the penultimate side-chain of the PDZ-bound OMP peptide and the L3 loop of the DegS protease domain play important roles in determining DegS activity via changes in active-site geometry and dynamics (Wilken et al., 2004; Hasselblatt et al., 2007). Distinguishing between these models is important for understanding molecular mechanism and has implications for understanding how regulation of DegS activity has evolved, for modeling the envelope-stress response

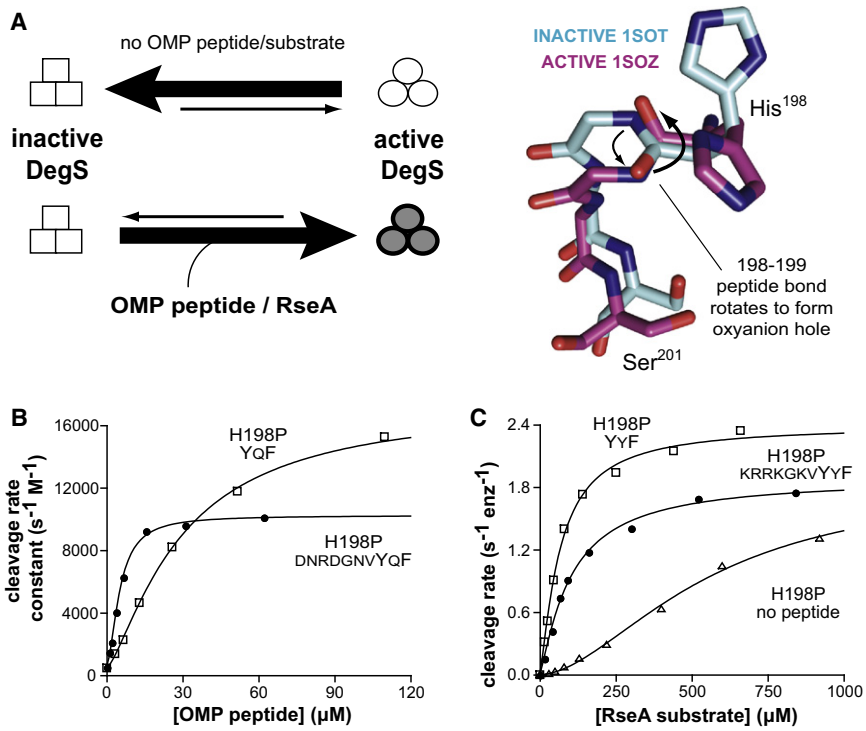

Figure 1. Allosteric Activation of DegS and the H198P Mutant

(A) The DegS trimer equilibrates between inactive (squares) and active conformations (circles), with OMP-peptide and RseA-substrate binding stabilizing the active enzyme. Activation involves rotation of the peptide bond between His^{198} and Gly^{199} to create a functional oxyanion hole (Wilken et al., 2004).

(B) Activation of H198P DegS (0.2 μM trimer) cleavage of RseA (50 μM) by the DNRDGNVYQF and YQF peptides. The lines are fits to the equation rate = basal + max/(1+(K_{act}/[peptide])^n), where basal is the unstimulated cleavage rate, max is the maximal cleavage rate, K_{act} is the activation constant, and n is the Hill constant. Fitted parameters are listed in Table 1.

(C) Substrate dependence of the steady-state rate of RseA cleavage by H198P DegS (0.2 μM trimer) without OMP peptide, with saturating KRRKGKVYYF peptide (60 μM), or with saturating YYF peptide (230 μM). The lines are fits to the Hill form of the Michaelis-Menten equation: rate = V_{max}/(1+(K_M/[RseA])^n). Fitted constants are listed in Table 1.

in vivo, and for engineering this and related proteolytic systems for alternative uses.

Here, we report biochemical and structural experiments that probe DegS activation. We find that a single mutation in the active site (H198P) partially bypasses the normal requirement for OMP-peptide activation. When the H198P mutation is combined with additional mutations that disrupt inhibitory interactions between the PDZ domain and the protease domain, the need for peptide activation is almost completely abolished, and RseA binding alone stimulates the mutant to activity levels similar to those of peptide-activated wild-type DegS. These mutations, OMP-peptide binding, and covalent active-site modification of DegS all act in concert to stabilize the active enzyme. Finally, we present crystal structures that reveal how the H198P mutation stabilizes active DegS and show that specific contacts between bound OMP peptides and the protease domain are not required for allosteric activation of DegS.

RESULTS

The H198P Mutation Activates DegS in the Absence and Presence of OMP Peptide

The allosteric switch between the inactive and active conformations of DegS changes the oxyanion-hole of the enzyme from a malformed to a catalytically competent structure (Figure 1A; Wilken et al., 2004; Zeth, 2004; Sohn et al., 2007; Hasselblatt et al., 2007). In this switch, the His^{198}-Gly^{199} peptide bond rotates almost 180°, allowing the -NH to accept a hydrogen bond from the carbonyl oxygen of the substrate scissile peptide bond. Residue 198 is poorly conserved in the family of HtrA proteases. For example, proline occupies this position in DegS homologs from *Mycobacterium tuberculosis* and *Pseudomonas aeruginosa*, and these proteases may be somewhat more active than DegS in the absence of activating ligands (Mohamedmohaideen et al., 2008; Cezairliyan and Sauer, 2009). Thus, we hypothesized that residue 198 might influence the conformation of the DegS oxyanion hole.

We substituted His^{198} with alanine or proline. The H198A mutant behaved like wild-type DegS in assays of RseA cleavage and OMP-peptide stimulation (not shown). By contrast, the H198P variant displayed properties expected if this mutation substantially increases the fraction of active DegS molecules in the absence of OMP peptide, but still results in most unliganded enzymes assuming the inactive conformation. Multiple experiments supported this conclusion. (*i*) In assays using sub-K_M concentrations of RseA with no OMP peptide, the H198P variant cleaved RseA 150-fold faster than did wild-type DegS (Table 1). This result suggests that a much higher fraction of mutant than wild-type enzymes is active in the absence of OMP peptide. (*ii*) Addition of saturating YQF OMP peptide enhanced H198P cleavage activity by an additional factor of 20-fold (Figure 1B; Table 1), demonstrating that most peptide-free H198P enzymes remain in the inactive conformation. Under comparable conditions of YQF saturation, the H198P mutant was also about 7-fold more active than wild-type DegS (Table 1), suggesting that most peptide-bound wild-type enzymes are still inactive when RseA concentrations are low. Similar results were obtained with saturating concentrations of two other OMP peptides (KRRKGKVYYF and DNRDGNVYYF), although the degrees of stimulation varied for each OMP peptide (Table 1). Previous studies suggest that this disparity occurs because different OMP peptides bind active and inactive DegS with varying affinities (Sohn and Sauer, 2009). (*iii*) The OMP-peptide concentrations required for half-maximal stimulation of activity (K_{act}) were lower for the H198P enzyme

Table 1. Properties of DegS Variants in RseA Cleavage and OMP-Peptide Binding

		Activation Parameters		
DegS Variant	OMP Peptide	Maximum Activity ($M^{-1}s^{-1}$)	K_{act} (μM)	Hill Constant
Wild-type	None	*2.9 ± 0.5*	n.a.	n.a.
Wild-type	YQF	*2100 ± 200*	*260 ± 10*	*1.6 ± 0.1*
Wild-type	DNRDGNVYQF	*590 ± 70*	*50 ± 5*	*1.6 ± 0.1*
Wild-type	KRRKGKVYYF	*70 ± 7*	*≤1 μM*	*~1.2*
H198P	None	510 ± 70	n.a.	n.a.
H198P	YQF	14400 ± 2000	29 ± 5	1.3 ± 0.1
H198P	DNRDGNVYQF	11400 ± 1500	4.4 ± 0.6	1.4 ± 0.1
H198P	KRRKGKVYYF	10400 ± 1200	n.d.[a]	n.d.[a]
H198P/K243D	None	9500 ± 920	n.a.	n.a.
H198P/K243D	DNRDGNVYYF	12800 ± 1700	n.d.[a]	n.d.[a]
H198P/D320A	None	9700 ± 960	n.a.	n.a.
H198P/D320A	YQF	17900 ± 1200	n.d.[a]	n.d.[a]
H198P/D320A	DNRDGNVYYF	12300 ± 1100	n.d.[a]	n.d.[a]
		Michaelis-Menten Parameters		
DegS Variant	OMP Peptide	V_{max} (s^{-1} enz^{-1})	K_M (μM)	Hill Constant
Wild-type	DNRDGNVYYF	*1.1 ± 0.2*	*750 ± 120*	*1.6 ± 0.2*
Wild-type	YYF	*2.6 ± 0.2*	*370 ± 40*	*1.4 ± 0.2*
H198P	None	1.4 ± 0.3	560 ± 40	1.6 ± 0.1
H198P	YQF	2.2 ± 0.1	69 ± 3	1.2 ± 0.2
H198P	YYF	2.3 ± 0.1	64 ± 3	1.3 ± 0.1
H198P	DNRDGNVYYF	2.0 ± 0.2	94 ± 8	1.2 ± 0.1
H198P	KRRKGKVYYF	2.0 ± 0.1	130 ± 20	1.1 ± 0.1
H198P/K243D	None	1.2 ± 0.1	70 ± 5	1.2 ± 0.1
H198P/K243D	DNRDGNVYYF	1.8 ± 0.2	68 ± 3	1.2 ± 0.1
H198P/D320A	None	1.6 ± 0.2	110 ± 10	1 1 ± 0.1
H198P/D320A	YQF	2.3 ± 0.2	61 ± 4	1.0 ± 0.1
H198P/D320A	DNRDGNVYYF	2.0 ± 0.1	101 ± 2	1.1 ± 0.1
	OMP Peptide Binding[b]			
DegS Variant	K_D (μM)			
PDZ domain	*0.6 ± 0.2*			
Wild-type	*4.6 ± 0.3*			
DFP wild-type	2.0 ± 0.1			
H198P	1.9 ± 0.1			
DFP-H198P	0.39 ± 0.05			
K243D	3.1 ± 0.4			
H198P/K243D	0.68 ± 0.02			
D320A	1.1 ± 0.1			
H198P/D320A	0.45 ± 0.04			
DFP-H198P/D320A	0.31 ± 0.03			

Activation parameters were determined using sub-K_M concentration of substrate by experiments like those shown in Figure 1B. Values in italics are from Sohn and Sauer (2009). n.d., not determined; n.a., not applicable.

[a] Complete titration curves were not determined, but near saturation was confirmed by testing at least two peptide concentrations that differed by a 2-fold minimum.

[b] The binding affinities are for the peptide fluorescein-β-alanine-KKDNRDGNYYF. Experimental values are an average of two or more independent determinations. Errors were calculated as $\sqrt{1/(n-1)\sum_1^n (value - mean)^2}$, where n is the number of independent trials.

than for wild-type DegS, and the Hill coefficients for peptide activation were also slightly smaller for the mutant (Table 1). Both results indicate that the free-energy gap between active and inactive DegS is smaller for H198P than for the wild-type enzyme.

Activation by Substrate Binding

The binding of RseA substrate to wild-type DegS helps stabilize the active enzyme (Sohn and Sauer, 2009). To address this issue for the H198P variant, we assayed rates of RseA cleavage at

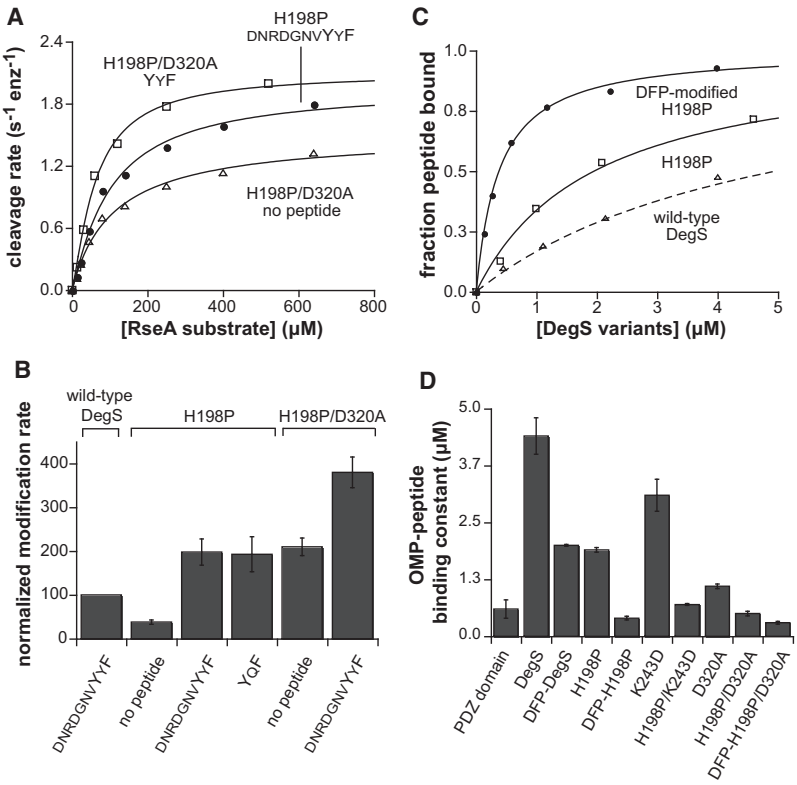

Figure 2. The H198P Mutation Stabilizes Active DegS Synergistically with Other Mutations and Active-Site Modification

(A) Substrate dependence of the steady-state rate of RseA cleavage by H198P/D320A DegS (0.1 μM trimer) without OMP peptide, with saturating DNRDGNVYYF peptide (30 μM), or with saturating YYF peptide (130 μM). The lines are fits to the Hill form of Michaelis-Menten equation.

(B) Rates of rh-FP modification of wild-type, H198P DegS, and H198P/D320A DegS without OMP peptide or with saturating OMP peptides. The rates are normalized to an arbitrary value of 100 for the wild-type enzyme plus DNRDGNVYYF peptide (Sohn and Sauer, 2009). Errors bars were calculated as $\sqrt{1/(n-1)\sum_1^n (value - mean)^2}$, where n is the number of independent trials.

(C) DegS, H198P DegS, or DFP-modified H198P DegS binding to the OMP-peptide fluorescein-β-alanine-KKDNRDGNYYF (30 nM) was monitored by changes in fluorescence anisotropy. The data were fitted to a quadratic equation for a 1:1 binding isotherm.

(D) Binding affinities of different DegS variants for the fluorescein-β-alanine- KKDNRDGNYYF OMP peptide. Errors bars were calculated as described above.

different substrate concentrations either with or without saturating OMP peptide (Figure 1C). Without peptide, high substrate concentrations resulted in robust H198P cleavage activity, albeit with a relatively high K_M (560 μM) and a Hill constant (1.6) indicative of substantial positive cooperativity. With saturating concentrations of different OMP peptides, V_{max} for RseA cleavage by H198P was only 40%–60% higher than without peptide, and both the K_M (64–130 μM) and Hill constants (1.1–1.3) were lower (Table 1; Figure 1C). These results indicate that RseA binding alone is sufficient to activate a majority of H198P enzymes, although conversion of the peptide-free enzyme to the active conformation is energetically more costly and thus more cooperative than that of the peptide-bound enzyme. The latter results are consistent with a model in which both OMP-peptide binding and substrate binding contribute to stabilizing the active enzyme.

Of the OMP peptides tested, saturating YYF resulted in the highest maximal rates of RseA cleavage both for wild-type DegS (2.6 ± 0.2 s^{-1} enz^{-1}; Sohn and Sauer, 2009) and for the H198P variant (2.3 ± 0.1 s^{-1} enz^{-1}; Table 1). Because these V_{max} values are within error of each other, it is likely that the functional conformations of the wild-type and mutant enzymes are almost equally active in RseA cleavage. As a result, the observed differences in activation by OMP peptides or RseA substrate almost certainly arise because adopting the active conformation is less energetically costly for the mutant than for the wild-type enzyme.

Additivity of H198P and Other Allosteric Mutations

The D320A and K243D mutations disrupt salt bridges between the DegS PDZ domain and protease domain and result in higher levels of peptide-independent protease activity (Sohn et al., 2007; Sohn and Sauer, 2009). When we combined H198P with either D320A or K243D, the resulting double mutants were even more active than H198P alone in cleaving sub-K_M concentrations of RseA in the absence of OMP peptide (Table 1). Moreover, without peptide, the concentration of RseA required for half-maximal cleavage by H198P/K243D DegS (70 μM) or H198P/D320A DegS (110 μM) was substantially lower than for H198P DegS (560 μM) (Table 1; Figure 2A), and the Hill constants for substrate activation were significantly lower for the double mutants (1.1–1.2) than for H198P alone (1.6). We conclude that the fraction of active enzymes is higher for the double mutants than for H198P in the absence of OMP peptide but is still less than 1. In the presence of saturating concentrations of different OMP peptides, V_{max} for the double mutants was essentially the same as for H198P alone (Table 1; Figure 2A).

Active-Site Reactivity

As an additional activity test, we monitored reactivity with rhodamine-fluorophosphate (rh-FP), which modifies Ser^{201} in the active site of DegS only when the oxyanion hole is properly formed. For example, rh-FP modified wild-type DegS at a detectable rate in the presence but not the absence of OMP peptides (Sohn and Sauer, 2009). By contrast, without OMP peptides, we observed a modest rate of rh-FP modification of H198P DegS and a higher rate of modification of H198P/D320A DegS (Figure 2B). The rates of rh-FP modification of both variants were increased in the presence of OMP peptides (Figure 2B). These results support a model in which the H198P mutation increases the fraction of enzymes that assume the active conformation in the absence of OMP peptides, and that this fraction is

Table 2. Crystallographic Data and Refinement Statistics

OMP Peptide	YQF	YRF	DNRDGNVYYF	DNRDGNVYQF
Crystal form	Form-1	Form-1	Form-2	Form-2
PDB code	3GDV	3GDU	3GDS	3GCO
Space group	$C222_1$	$C222_1$	$P2_13$	$P2_13$
Unit cell	a = 118.88 Å	a = 117.57 Å	a = 118.82 Å	a = 119.41 Å
	b = 172.28 Å	b = 171.28 Å	b = 118.82 Å	b = 119.41 Å
	c = 114.77 Å	c = 111.69 Å	c = 118.82 Å	c = 119.41 Å
Resolution	2.49 Å	2.93 Å	2.85 Å	2.80 Å
Wavelength	0.97918 Å	0.97918 Å	1. 5418 Å	1.5418 Å
R_{sym}	0.080 (0.24)	0.069 (0.439)	0.075 (0.54)	0.091 (0.846)
Unique reflections	39897 (3210)	22787 (2210)	13350 (1313)	14287(1415)
Completeness (%)	96.4 (79.1)	94.9 (93.5)	99.9 (99.9)	98.9 (100)
Data redundancy	4.3 (3.9)	4.0 (2.8)	9.2 (7.9)	11.6 (8.1)
I/σI	19.97	19.5	31.18	29.5
R_{cryst}	0.191 (0.205)	0.209 (0.271)	0.209 (0.264)	0.211 (0.273)
R_{free}	0.224 (0.255)	0.231 (0.324)	0.221 (0.377)	0.239 (0.302)
Rmsd bond length (Å)	0.005	0.003	0.004	0.003
Rmsd bond angle (°)	0.830	0.590	0.805	0.715
Solvent atoms	143	0	0	0
Average B value	73.7	125.2	63.3	84.6
Ramachandran favored/allowed (%)	98.2/100	97.4/100	97.0/100	96.6/100

$R_{sym} = S_h S_j |I_j(h) - < I(h) > | / S_h S_j < I(h) >$, where $I_j(h)$ is the j^{th} reflection of index h and < I(h) > is the average intensity of all observations of I(h). $R_{work} = S_h |F_{obs}(h) - F_{calc}(h)| | / S_h |F_{obs}(h)|$, calculated over the 95% of the data in the working set. R_{free} equivalent to R_{work} except calculated over the 5% of the data assigned to the test set.
Numbers in parentheses represent values for the highest-resolution bin.

increased further both by OMP-peptide binding and by additional activating mutations.

DFP Modification Stabilizes the Active Conformation of DegS

OMP peptides bind preferentially to the active DegS conformation (Sohn and Sauer, 2009). Thus, peptide-binding affinity provides an independent probe of DegS conformation, because variants with a higher equilibrium fraction of active enzyme should bind more tightly. Peptide affinity also provides a method of assessing the conformational effects of active-site modification by di-isopropylfluorophosphate (DFP). By monitoring fluorescence anisotropy of a fluorescein-labeled OMP peptide, we assayed binding at increasing concentrations of mutant and/or DFP-modified enzymes (Table 1; Figures 2C and 2D). In each case, the DFP-modified enzyme bound more tightly than the corresponding unmodified enzyme. For example, H198P DegS bound peptide with an affinity of 1.9 μM, whereas DFP-modified H198P bound with an affinity of 0.39 μM. In general, the peptide affinities mirrored results based on activity measurements, with stronger binding being facilitated independently by the H198P, K243D, and D320A mutations. The tightest peptide binding was obtained using DFP-modified H198P/D320A, suggesting that a higher fraction of this enzyme adopts the active conformation than for any of the other variants tested.

Crystal Structures of Peptide-Bound DegS

We crystallized DFP-modified H198P/D320A DegS in space group $C222_1$ (form 1) or $P2_13$ (form 2) with four different OMP peptides. In total, we obtained two form-1 crystals (with peptides YQF or YRF) and two form-2 crystals (with peptides DNRDGNVYQF, or DNRDGNVYYF). In each case, we solved the structure by molecular replacement. Table 2 lists crystal parameters and refinement statistics. In the form-1 crystals, there was one DegS trimer in the asymmetric unit. In the form-2 crystals, the asymmetric unit contained one subunit, and the trimer was generated by crystal symmetry. In our structures and the peptide-bound 1SOZ structure (Wilken et al., 2004), the core elements of the protease domains were essentially identical to each other, with root-mean-square deviation (rmsd) values $\leq$ 0.42 Å for 163 Cα positions (Table 3). The structures of the trimers were also very similar. For example, the 1SOZ trimer superimposed on our YRF-bound trimer with an rmsd of 0.44 Å for 489 Cα positions.

Because our DegS variants had been treated with DFP prior to crystallization, we expected that the active-site serine (Ser^{201}) would be modified. Indeed, the electron-density maps revealed the presence of monoisopropylphosphorylserine (Mis^{201}) in each subunit (Figure 3). The second isopropyl group of DFP was presumably removed by hydrolysis. The O1P oxygen of Mis^{201} occupied the oxyanion hole of the active site, making good hydrogen bonds to the main-chain -NH groups of residue 199 (2.75 ± 0.05 Å) and residue 201 (2.93 ± 0.19 Å) and a weaker interaction with the -NH of residue 200 (3.38 ± 0.27 Å; Figure 3B). DegS cleavage of RseA occurs at a Val-Ser peptide bond (Walsh et al., 2003), and the isopropyl group of Mis^{201} is a proxy for the valine side chain of the substrate in the acyl-enzyme. This isopropyl group sits in the S1-specificity pocket of DegS, which is formed by the side chains of Ile^{196}, Leu^{218}, and Ser^{219}

Table 3. Structural Comparison of Protease Domains

	3GDV_A	3GDV_B	3GDV_C	1SOZ_A	1SOZ_B	1SOZ_C	3GDU_A	3GDU_B	3GDU_C	3GDS_A	3GCO_A
	Rmsd Å	Rmsd Å	Rmsd Å	Rmsd Å	Rmsd Å	Rmsd Å	Rmsd Å	Rmsd Å	Rmsd Å	Rmsd Å	Rmsd Å
3GDV_A	0.00										
3GDV_B	0.32	0.00									
3GDV_C	0.28	0.22	0.00								
1SOZ_A	0.29	0.38	0.36	0.00							
1SOZ_B	0.27	0.30	0.27	0.30	0.00						
1SOZ_C	0.30	0.33	0.28	0.30	0.26	0.00					
3GDU_A	0.31	0.42	0.38	0.36	0.35	0.39	0.00				
3GDU_B	0.41	0.28	0.33	0.41	0.37	0.39	0.39	0.00			
3GDU_C	0.38	0.33	0.25	0.41	0.34	0.34	0.37	0.27	0.00		
3GDS_A	0.25	0.24	0.18	0.31	0.24	0.28	0.34	0.32	0.27	0.00	
3GCO_A	0.25	0.26	0.20	0.33	0.25	0.29	0.34	0.34	0.30	0.14	0.00

The core protease domains (residues 44–63, 79–133, 138–176, 190–216, and 229–250) of subunits in the 1SOZ, 3GDV, 3GDU, 3GDS, and 3GCO crystal structures of DegS were superimposed using 163 common Cα positions.

(Figure 3C). In our structures, these residues had somewhat different conformations than seen in peptide-free DegS or in the previously reported peptide-bound 1SOZ structure (Wilken et al., 2004; Zeth, 2004), suggesting that the some rearrangement of the S1 pocket is induced by the substrate mimic (Figure 3C). Notably, the S1 pocket in our structures was very similar to the corresponding region in a structure of the *M. tuberculosis* HtrA2 ortholog (rmsd = 0.4 Å), in which a peptide substrate was found acylated to the active-site serine (Mohamedmohaideen et al., 2008). Thus, our DFP-modified H198P/D320A structures mimic the substrate-bound enzyme.

Our crystal structures also suggest a mechanism by which the pyrrolidine ring of the mutant Pro^{198} side chain stabilizes the active conformation of DegS. A portion of the Pro^{198} ring contacts the aromatic ring of Tyr^{162} (Figure 3B), which is part of the LD loop and plays an important role in allosteric activation. During this process, the side chain and main chain of Tyr^{162} move from their positions in inactive DegS, allowing the Tyr^{162} backbone -NH to hydrogen bond to the main-chain carbonyl oxygen of residue 198, thereby stabilizing the functional oxyanion hole (Figure 3B; Wilken et al., 2004). As a result, the additional packing interactions between the side chains of Pro^{198} and Tyr^{162} in the H198P mutant could easily stabilize the active conformation of DegS relative to the inactive conformation (see Discussion).

Varied PDZ-Domain Positions

As observed in previous peptide-bound structures (Wilken et al., 2004; Hasselblatt et al., 2007), electron density for the PDZ

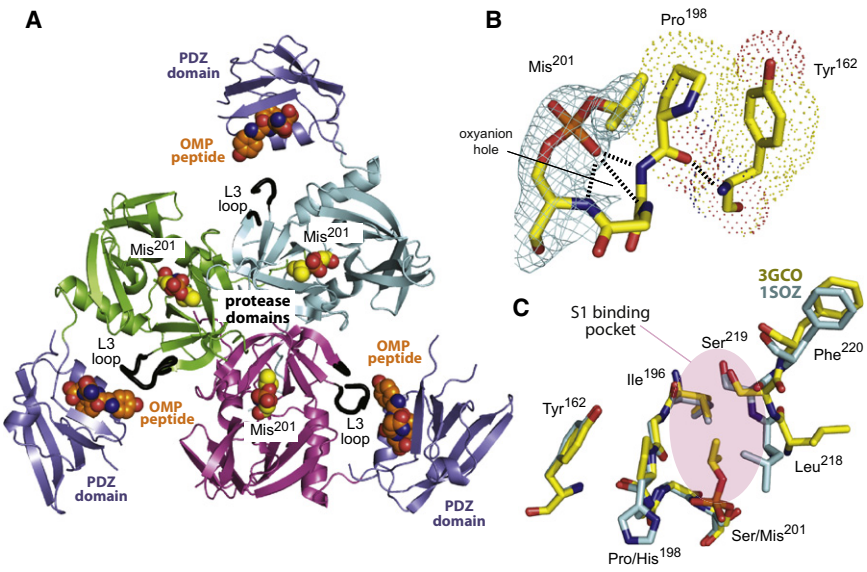

Figure 3. Structures

(A) Cartoon representation of the OMP-peptide bound H198P/D320A DegS trimer (3GDV). The protease domains of different subunits are colored green, cyan, and magenta, except the L3 loop, which is colored black; the PDZ domains are colored slate blue. The YQF OMP peptide and the modified active-site serine (Mis^{201}) are shown in CPK representation.

(B) Interactions near the active site of the 3GDV structure. The O1P oxygen of Mis^{201} ($2F_o$-F_c electron density contoured at 1.6 σ) accepts hydrogen bonds from the -NH groups of the oxyanion hole. Packing interactions between the pyrrolidine ring of Pro^{198} and the aromatic ring of Tyr^{162} help to stabilize the hydrogen bond between backbone carbonyl oxygen and -NH groups of these amino acids and therefore stabilize the functional active site.

(C) The peptide-bound 1SOZ structure (Wilken et al., 2004) and our peptide-bound 3GCO structure have very similar conformations near the active site, except for the modification of Ser^{201} in 3CGO and the $His^{198} \rightarrow Pro$ sequence change. In the 3GCO structure, Leu^{218} and Ser^{219} in the S1-specificity pocket move to some degree to accommodate the isopropyl moiety of Mis^{201}, which mimics the P1 side chain of a substrate.

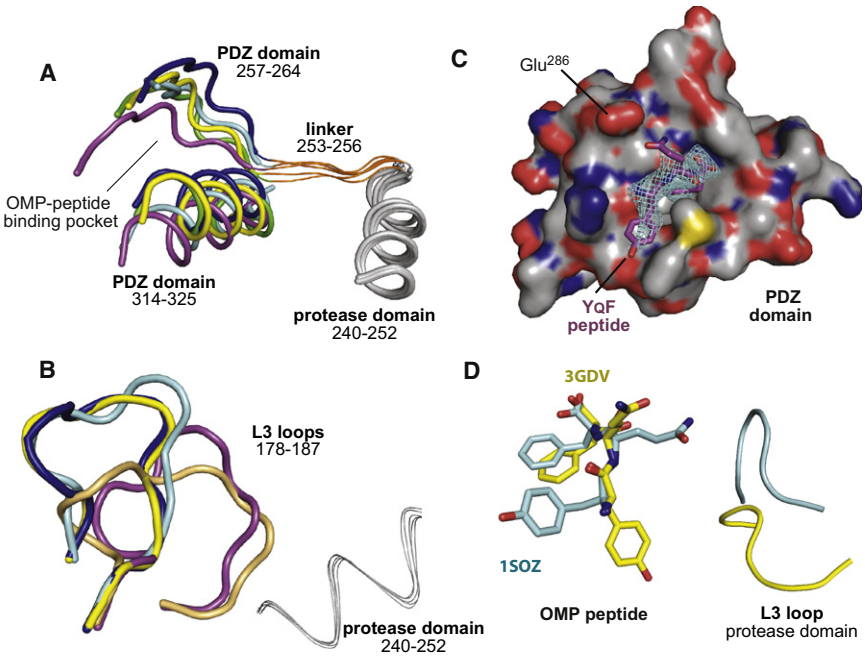

Figure 4. Structural Variations in PDZ Domains, L3 Loops, and OMP-Peptide Binding

(A) After alignment of the protease domains, the PDZ domains of different peptide-free structures (1TE0_A; magenta) and peptide-bound structures (1SOZ_B, cyan; 3GDV_A, yellow; 3GDV_B, green; 3GDS_A, blue) adopt somewhat different orientations. The linker that connects the protease and PDZ domains is colored in orange, and part of the aligned protease domain is shown in gray. Only parts of the PDZ domains are shown for simplicity.

(B) L3 loops assume variable conformations in the protease domains of different peptide-free structures (1SOT_B, light orange; 1TE0_A, magenta) and peptide-bound structures (1SOZ_B, cyan; 3GDV_A, yellow; 3GCO_A, blue). The last helix of the protease domain in these structures is also shown.

(C) Binding of the YQF OMP peptide (electron density for the OMP peptide from a simulated-annealing omit map is contoured at 1σ) to the PDZ domain of chain C in the 3GDV structure. The side chain of the penultimate peptide glutamine appears to hydrogen bond to Glu^{286} in the PDZ domain.

(D) Varied side-chain conformations and contacts between OMP peptides and the L3 loop. In subunit B of the 1SOZ structure, the penultimate peptide glutamine contacts the L3 loop and the antepenultimate tyrosine points away from the L3 loop. In subunit B of the 3GDV structure, the penultimate peptide glutamine makes no L3-loop contacts and the antepenultimate tyrosine is rotated approximately 90° from the 1SOZ position. This view was generated by aligning the OMP-peptide backbones.

domains (residues 256–355) in our structures was poorer than for the protease domains, but we built approximately 80% of each PDZ domain. The orientations of these PDZ domains with respect to their attached protease domains were roughly similar to those in prior structures (Wilken et al., 2004; Zeth, 2004; Hasselblatt et al., 2007). Namely, the helix formed by residues 314–325 in the PDZ domain, which forms part of the OMP-peptide binding site, was reasonably close to parts of the L3 loop in the protease domain and ran roughly parallel to the last helix (residues 240–252) of the protease-domain (Figures 3A and 4A).

Nevertheless, there were significant differences in the positioning of individual PDZ domains in different subunits and structures. Some of these differences are illustrated in Figure 4A. After superposition of the protease domains, poor alignment was observed among PDZ domains taken from our new structures and among PDZ domains from previously published peptide-bound and peptide-free structures. Differences in the positions of PDZ domains vis-à-vis the protease domain were observed even when the same OMP peptide was bound to this domain and even for peptide-bound PDZ domains in different subunits of a single crystallographic trimer. For example, comparing the same Cα positions in different PDZ domains revealed variations as large as 4 Å among our form-1 and form-2 structures, changes of 7 Å between some of our structures and previous peptide-bound structures, and movements of 10 Å between the most divergent peptide-bound and peptide-free structures.

In peptide-free DegS, the PDZ domain of each subunit mediates numerous polar and hydrophobic interactions with the corresponding protease domain, burying approximately 400 Å^2 of surface (Wilken et al., 2004; Zeth, 2004). The peptide-binding helix in the PDZ domain (residues 314–325; Figure 4A) makes many of these interactions with the protease domain. By contrast, the PDZ domains in our different peptide-bound structures made far fewer contacts with the protease domains and buried less surface (150 ± 60 Å^2). These peptide-mediated changes in interactions between the PDZ domain and the L3 loop occur because of movements in both structural elements. As observed for the PDZ domains, the L3 loops in different subunits of peptide-bound structures also adopted varied structures (Figure 4B).

Peptide Contacts

Each OMP peptide in our structures interacted with the PDZ domain largely as previously reported (Wilken et al., 2004). Specifically, the peptide α-carboxylate formed hydrogen bonds with the backbone -NH groups of residues 259 and 261 in the PDZ domain, the OMP-peptide backbone formed an irregular anti-parallel β sheet with PDZ residues 261–263, and the phenylalanine side chain of the C-terminal residue of the peptide packed into a deep hydrophobic pocket formed in part by residues in the 314–325 helix. However, significant differences in peptide-binding geometry were also observed. For example, the antepenultimate peptide tyrosine in all of our structures adopted a different rotamer than in the 1SOZ structure, as did the penultimate glutamine, when it was present in our structures (Figures 4C and 4D; Wilken et al., 2004).

Combining our new structures with those determined previously provides 14 independent views of peptide-bound DegS subunits, either in distinct crystal environments or with different OMP peptides bound. Among these structures, molecular contacts between the bound peptide and the protease domain varied widely and were sometimes completely absent. In

previous structures, a contact was observed between the penultimate side chain of the OMP peptide and the L3 loop in the protease domain (Wilken et al., 2004; Hasselblatt et al., 2007). By contrast, the penultimate side chains of the OMP peptides in our structures interacted only with residues in the PDZ domain. For example, in our form-1 crystal with bound YQF peptide, the glutamine side chain of the penultimate peptide residue interacts with the side chain of Glu^{286} in the PDZ domain. In a subset of our structures, contacts were seen between the antepenultimate peptide side chain and the L3 loop of the protease domain, but these interactions were highly variable.

DISCUSSION

Active DegS Structures

We were unable to obtain crystals of wild-type DegS in complex with OMP peptides, perhaps because wild-type DegS is largely in the inactive conformation even with saturating OMP peptide (Sohn and Sauer, 2009). By contrast, in trials using the DFP-modified H198P/D320A mutant, which is predominantly in the active conformation, crystals with OMP peptides were obtained under many different conditions, and four structures were solved. There are now a total of six peptide-bound DegS structures in different space groups or with different OMP peptides. Our new structures are of mutant proteins, whereas previous structures used a variant of "wild-type" DegS (Wilken et al., 2004; Hasselblatt et al., 2007). However, both peptide-bound wild-type structures crystallized in the same lattice as the inactive peptide-free enzyme, raising potential concerns about the influence of crystal packing on conformation. These wild-type DegS variants also lacked some N-terminal sequences that appear to stabilize the DegS trimer in our structures. In our view, the ensemble of structures provides the most accurate view of the conformational properties of DegS in the peptide-bound active structure.

In all of the peptide-bound DegS structures, the conformations of the core elements of the protease domain are essentially the same, and the oxyanion hole is properly formed. Indeed, in our new structures, an oxygen atom from the modified active-site serine mimics part of a substrate and accepts hydrogen bonds from the -NH groups of the oxyanion hole. The same core conformation of the protease domain is also observed in crystal structures of DegS lacking its PDZ domain (Hasselblatt et al., 2007; Sohn et al., 2007). Indeed, significant conformational differences in the protease domains of all of these structures are only observed in the LA, L2, and L3 loops, which are partially disordered in many subunits. Moreover, when these loops are fully ordered, they often make crystal-packing contacts.

The PDZ domains in all known "active" DegS structures have main-chain B-factors that are on average approximately twice those of the protease domains. Moreover, only 40%–85% of the PDZ residues are included in the models of different structures. The conformations of these structured parts and the mode of OMP-peptide binding are generally similar for different PDZ domains, but the orientations of the PDZ domains with respect to the attached protease domain differ substantially. As a consequence, wide variations are observed in contacts between the bound OMP peptides and the protease domains. In previous structures, contacts between the penultimate side chain of the OMP peptide and the L3 loop of the protease domain were observed (Wilken et al., 2004; Hasselblatt et al., 2007). Such interactions with the protease domain are absent in all of our structures, in which the penultimate side chain of the OMP peptide contacts the PDZ domain only. Indeed, when all of the peptide-bound structures are included, there are no conserved contacts between the OMP peptide and the protease domain and, in some cases, there are no interactions of any kind between these elements. Taken together, these observations suggest that the PDZ domains and bound OMP peptides in active DegS are only loosely tethered to the protease domains, with their exact orientations and contacts being determined predominantly by crystal packing. There is one structure of a peptide-bound DegS homolog, *M. tuberculosis* HtrA2 (Mohamedmohaideen et al., 2008). As in our DegS structures, no contacts are observed between the penultimate residue of the bound peptide and the protease domain in this HtrA2 structure.

Implications for Mechanisms of Allosteric Activation

There are two models for how OMP-peptide binding activates DegS. The inhibition-relief model posits that peptide binding breaks inhibitory interactions mediated by the PDZ domain, thereby shifting a dynamic equilibrium away from inactive DegS and toward the active enzyme (Walsh et al., 2003; Sohn et al., 2007; Sohn and Sauer, 2009). The peptide-activation model proposes that specific interactions between the penultimate side chain of the bound OMP peptide and the L3 loop of the protease domain are responsible for setting the precise level of DegS activity (Wilken et al., 2004). The most recent variation of this model states that "different activating peptides induce different rearrangements of loop L3, which have a different effect on the active site geometry and rigidity" (Hasselblatt et al., 2007). Thus, the first model proposes that there are two basic conformations of DegS, active and inactive, whereas the second model envisions a variety of functional conformations, each with a different activity (Figure 5).

Evidence supporting a peptide-activation-only model is weak. For example, contacts between the penultimate side chain of the PDZ-bound OMP peptide and the L3 loops vary within a given trimer in previously published structures and are absent in the structures reported here. Moreover, dramatic changes in the identity of the penultimate OMP-peptide residue result in only small changes in DegS activity (±15% from average) under conditions of peptide saturation (Sohn et al., 2007). Hence, contacts mediated by the penultimate side chain of the OMP peptide may have a 30% influence on DegS activity, but these effects are very small compared with effects at other peptide positions (up to 35-fold) and to the maximal levels of OMP-peptide activation of DegS (850-fold or greater; Sohn and Sauer, 2009).

How strong is the evidence for the inhibition-relief model? In this two-state equilibrium model, the unliganded enzyme is largely inactive because contacts between the PDZ domain and the protease domain stabilize inactive DegS. Preferential binding of OMP peptides and RseA substrate to active DegS then drive the equilibrium population toward this species (Sohn et al., 2007; Sohn and Sauer, 2009). As a consequence, any mutation that destabilizes inactive DegS or that stabilizes active DegS should result in higher peptide-independent activity. Both results are observed. The D320A and K243D mutations, which

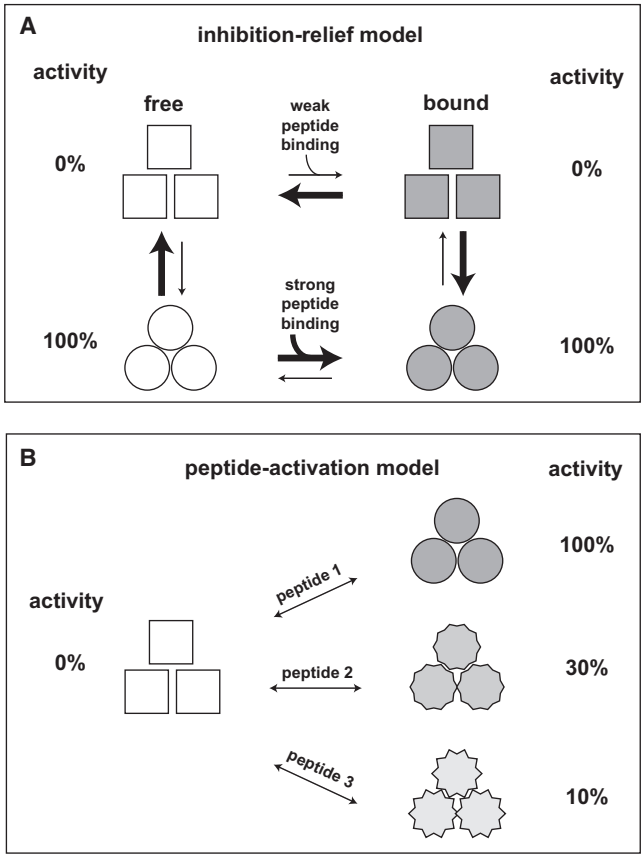

Figure 5. Models for DegS Activation

(A) The inhibition-relief model posits an equilibrium between free inactive trimers (open squares) and free active trimers (open circles). OMP peptides bind to both states (shaded circles or squares) and shift the equilibrium toward the active form because they bind more tightly to this conformation than the inactive conformation.

(B) The peptide-activation model posits that different OMP peptides stabilize slightly different DegS conformations, in which the precise activity depends on the identity of the penultimate side-chain of the bound peptide.

remove inhibitory salt bridges between the PDZ and protease domains, activate DegS (Sohn et al., 2007; Sohn and Sauer, 2009). As we have shown here, so does the H198P mutant, which makes additional stabilizing interactions in the active conformation. Combining either D320A or K243D with H198P resulted in double mutants that cleaved low concentrations of RseA 20-fold to 100-fold faster than the single mutants in the absence of OMP peptides. In fact, subsequent addition of saturating OMP peptides stimulated the protease activity of the double mutants less than 2-fold. Synergy was also observed in OMP-peptide binding, which was stronger for the H198P/D320A or H198P/K243D double mutants than for the single mutants and stronger for DFP-modified H198P and the double mutants than for the unmodified enzymes. Thus, mutations/modifications that stabilize the active enzyme or that destabilize the inactive enzyme have additive effects, as expected for a two-state allosteric model.

The inhibition-relief model obeys the rules of MWC allostery (Monod et al., 1965). Thus, activity can be predicted from the equilibrium constant that relates the unliganded inactive and active species and from the concentrations and affinities of OMP peptide and substrate for both enzyme conformations. Previously, we showed that the experimental behavior of numerous variants of DegS with multiple OMP peptides could be reproduced quantitatively using the MWC model (Sohn and Sauer, 2009). For example, saturating concentrations of different OMP peptides activate DegS to very different maximal levels, which the inhibition-relief model explains by affinity-driven changes in the equilibrium distribution of active and inactive enzymes with bound peptide (Figure 5A). By contrast, the peptide-activation model explains such differences in peptide activity by changes in the conformation or dynamics of the functional enzyme (Figure 5B). The inhibition-relief model explains why the cooperativity of activation changes for different peptides, how different peptides change V_{max} and K_M for substrate cleavage, and why peptides, which activate wild-type DegS poorly, can be much better activators of mutants in which the inactive conformation is destabilized. The peptide-activation model cannot explain many of these results or can only account for them in an ad hoc manner. One might argue that the observation of variable peptide-bound PDZ domain orientations and modest differences in protease-domain loop conformations in different crystal structures of active DegS argues against a strict two-state model. However, OMP-peptide binding in the inhibition-relief model serves only to break restraining contacts, and thus a specific active conformation of the peptide-bound PDZ domain is not required. More importantly, if the observed variations in structure are nearly isoenergetic, then the system will still behave in a two-state fashion.

The H198P Mutation and Allosteric Activation

The H198P mutation appears to shift the allosteric equilibrium toward the active enzyme. Compared with wild-type DegS, for example, H198P DegS shows a much higher RseA cleavage rate without OMP peptides, binds activating peptides more tightly, and displays smaller Hill coefficients for substrate and OMP peptides. Modification of the active-site serine by covalent inhibitors also occurs at a faster rate for the H198P mutant than for wild-type DegS.

For wild-type DegS, the equilibrium ratio of the inactive to active conformations is about 15,000:1 in the absence of OMP peptide and substrate, corresponding to a free-energy difference of approximately 6 kcal/mol (Sohn and Sauer, 2009). Fitting of the H198P experimental data to equations for MWC allostery gave an equilibrium ratio of unliganded inactive to active species of 22:1, corresponding to a free energy difference of roughly 2 kcal/mol (not shown). This reduction predicts that even modest stabilization via OMP peptide and/or substrate binding should now be sufficient to shift the equilibrium so that active H198P species predominate. Indeed, we observed that high concentrations of the RseA substrate alone were able to activate H198P DegS to levels about 60% of those achieved with the best OMP-peptide activation. By contrast, for wild-type DegS, cleavage of high concentrations of RseA in the absence of OMP peptide occurs at a rate less than 0.3% of the peptide-stimulated value.

How does the H198P mutation increase the equilibrium fraction of active DegS? In our crystal structures, the pyrrolidine

ring of Pro^{198} packs closely against the aromatic ring of Tyr^{162} (Figure 3B). Specifically, the Cγ and Cδ proline methylene groups make numerous van der Waals contacts with the tyrosine ring. These interactions were absent when we modeled Pro^{198} into inactive DegS and corresponding contacts made by His^{198} are absent in both active and inactive wild-type DegS (Wilken et al., 2004; Zeth, 2004). Allosteric activation of DegS involves movement of Tyr^{162} to allow its main-chain -NH to hydrogen bond to the carbonyl oxygen of residue 198. This interaction, in turn, locks the main-chain -NH of Gly^{199} into the functional oxyanion-hole conformation. Thus, the extra packing interactions between Pro^{198} and Tyr^{162} should stabilize active DegS relative to inactive DegS. To account quantitatively for the 4 kcal/mol shift in favor of the active conformation of H198P, the new van der Waals interactions mediated by Pro^{198} would need to stabilize each active subunit of the trimer by approximately 1.3 kcal/mol relative to each inactive subunit.

Allosteric activation mediated by ligand binding requires DegS to adopt alternative inactive and active structures with an energy gap large enough to keep the unliganded protease predominantly in the inactive state. Different orthologs probably use diverse types of interactions to stabilize the inactive state, but the structures of the active protease domains of these enzymes must be constrained by the need to bind substrate and catalyze peptide-bond cleavage. We anticipate that other members of the HtrA-protease family will share this ligand-mediated regulatory mechanism. From a biological and evolutionary perspective, this relief of inhibition mechanism is highly robust because it allows DegS function to be tuned to any desired level of fractional activity simply by evolving OMP peptides with appropriate affinities for the active and inactive enzyme conformations.

EXPERIMENTAL PROCEDURES

Proteins and Peptides

Wild-type and mutant variants of *E. coli* DegS (residues 27–355) contained an N-terminal His_6 tag and lacked the membrane anchor. Mutations were generated by the QuikChange method (Stratagene) and confirmed by DNA sequencing. DegS variants and a ^{35}S-labeled variant of the periplasmic domain of *E. coli* RseA (residues 121–216) with a C-terminal His_6 tag were expressed, purified, and stored as described elsewhere (Walsh et al., 2003; Sohn et al., 2007; Sohn and Sauer, 2009). All DegS variants eluted as trimers in the gel-filtration step of purification (Superdex 200). Peptides were synthesized by the MIT Biopolymer Laboratory, purified by high-pressure liquid chromatography, and their expected molecular mass was confirmed by matrix-assisted laser desorption/ionization time-of-flight mass spectrometry.

Enzymatic and Biochemical Assays

All assays were performed at room temperature (23°C ± 1°C) using conditions described previously (Sohn et al., 2007; Sohn and Sauer, 2009). For cleavage assays, ^{35}S-RseA was incubated with DegS or mutants for different times, and acid-soluble radioactivity was quantified by scintillation counting. The binding of DegS or mutant variants to a fluorescent OMP peptide was assayed by monitoring changes in fluorescence anisotropy (excitation 480 nm; emission 520 nm), after correction for protein scattering. DFP modification of wild-type DegS was performed with saturating OMP peptide. No peptide was needed for full modification of the H198P and H198P/D320A mutants. OMP peptides and/or unincorporated DFP were removed by Ni-NTA chromatography and dialysis. All of the DFP-modified enzymes showed no detectable RseA cleavage. Binding curves, Michaelis-Menten curves, and peptide-activation curves were fitted to appropriate equations using the nonlinear least-squares subroutine in KaleidaGraph (Synergy software). Rh-FP (Liu et al., 1999) was a gift from C. Salisbury, E. Weerapana, and B. Cravatt (Scripps Institute). Modification of DegS or variants (0.9 μM trimer) with rhodamine-FP (20 μM) was performed in the presence or absence of OMP peptides as described (Sohn and Sauer, 2009).

Crystallization

H198P/D320A DegS (150 μM trimer) was incubated with 20 mM DFP at room temperature for 2 hr, 20 mM fresh DFP was added, incubation was continued overnight, and the mixture was dialyzed against 50 mM HEPES (pH 7.4), 100 mM NaCl. A 2-fold molar excess of OMP peptide was added prior to initial robotic high-throughput crystallization trials using Index screen (Hampton Research), ProComplex, PACT suite (QIAGEN), and JCSG+Suite (QIAGEN). Several crystal hits were obtained within one week at 20°C. Form-1 crystals grew with 4% PEG-6000, 150 mM $MgCl_2$, and 100 mM Tris (pH 6.0). Form-2 crystals grew with 3% PEG-3350, 150 mM NaF, and 100 mM Bis-Tris propane (pH 6.5). For cryo-protection, an equal volume of 40% MPD in well solution was added to the drop just prior to freezing in liquid nitrogen. Diffraction data for two form-1 crystals were collected at the NE-CAT 24-ID-C beamline at the Argonne National Labs Advanced Photon Source. Form-2 crystal data were collected in house using a Rigaku MicroMax008-HP rotating source. Initial phases were obtained by molecular replacement using PHASER (Storoni et al., 2004) and the peptide-free DegS (1SOT, 1TE0) and/or DegS-ΔPDZ (2QF) structures as search models. Positive electron density for OMP peptides was observed in the initial molecular-replacement maps. Final structures were refined by reiterative model building using COOT (Emsley and Cowtan, 2004) and refinement using PHENIX (Adams et al., 2002). Peptide positions in the final structures were confirmed by simulated-annealing omit maps.

ACCESSION NUMBERS

Structures of the DegS protease in complex with OMP peptides have been deposited in the Protein Data Bank with the accession codes 3GDV, 3GDU, 3GDS, and 3GCO.

ACKNOWLEDGMENTS

We thank C. Salisbury, E. Weerapana, and B. Cravatt for the gift of rhodamine-FP; J. Whittle and T. Schwartz for data collection at APS; and E. Gur and S. Kim for helpful discussions. Supported by NIH grant AI-16892. J. Sohn was supported by an NIH postdoctoral fellowship (F32AI-074245-01A1). Studies at the NE-CAT beamlines of the Advanced Photon Source were supported by NIH-NCRR award RR-15301 and by the DOE Office of Basic Energy Sciences under contract DE-AC02-06CH11357.

Received: June 17, 2009
Revised: July 25, 2009
Accepted: July 30, 2009
Published: October 13, 2009

REFERENCES

Adams, P.D., Grosse-Kunstleve, R.W., Hung, L.W., Ioerger, T.R., McCoy, A.J., Moriarty, N.W., Read, R.J., Sacchettini, J.C., Saurter, N.K., and Terwilliger, T.C. (2002). PHENIX: building new software for automated crystallographic structure determinaion. Acta Crystallogr. D Biol. Crystallogr. *58*, 1948–1954.

Ades, S.E. (2008). Regulation by destruction: design of sigmaE envelope stress response. Curr. Opin. Microbiol. *11*, 535–540.

Ades, S.E., Connolly, L.E., Alba, B.M., and Gross, C.A. (1999). The *Escherichia coli* sigma E -dependent extracytoplasmic stress response is controlled by the regulated proteolysis of an anti-sigma factor. Genes Dev. *13*, 2449–2461.

Alba, B.M., and Gross, C.A. (2004). Regulation of the *Escherichia coli* sigma-dependent envelope stress response. Mol. Microbiol. *52*, 613–619.

Alba, B.M., Leeds, J.A., Onufryk, C., Lu, C.Z., and Gross, C.A. (2002). DegS and YaeL participate sequentially in the cleavage of RseA to activate the sigma E -dependent extracytoplasmic stress response. Genes Dev. *16*, 2156–2168.

Baslé, A., Rummel, G., Storici, P., Rosenbusch, J.P., and Schirmer, T. (2006). Crystal structure of osmoporin OmpC from *E. coli* at 2.0 Å. J. Mol. Biol. *362*, 933–942.

Cezairliyan, B.O., and Sauer, R.T. (2009). Control of *Pseudomonas aeruginosa* AlgW protease cleavage of MucA by peptide signals and MucB. Mol. Microbiol. *72*, 368–379.

Chaba, R., Grigorova, I.L., Flynn, J.M., Baker, T.A., and Gross, C.A. (2007). Design principles of the proteolytic cascade governing the sigmaE-mediated envelope stress response in Escherichia coli: Keys to graded, buffered, and rapid signal transduction. Genes Dev. *21*, 124–136.

Ehrmann, M., and Clausen, T. (2004). Proteolysis as a regulatory mechanism. Annu. Rev. Genet. *38*, 709–724.

Emsley, P., and Cowtan, K. (2004). Coot: model-building tools for molecular graphics. Acta Crystallogr. D Biol. Crystallogr. *60*, 2126–2132.

Flynn, J.M., Levchenko, I., Sauer, R.T., and Baker, T.A. (2004). Modulating substrate choice: the SspB adaptor delivers a regulator of the extracytoplasmic-stress response to the AAA+ protease ClpXP for degradation. Genes Dev. *18*, 2292–2301.

Grigorova, I.L., Chaba, R., Zhong, H.J., Alba, B.M., Rhodius, V., Herman, C., and Gross, C.A. (2004). Fine-tuning of the Escherichia coli sigmaE envelope stress response relies on multiple mechanisms to inhibit signal-independent proteolysis of the transmembrane anti-sigma factor, RseA. Genes Dev. *18*, 2686–2697.

Hasselblatt, H., Kurzbauer, R., Wilken, C., Krojer, T., Sawa, J., Kurt, J., Kirk, R., Hasenbein, S., Ehrmann, M., and Clausen, T. (2007). Regulation of the sigmaE stress response by DegS: how the PDZ domain keeps the protease inactive in the resting state and allows integration of different OMP-derived stress signals upon folding stress. Genes Dev. *21*, 2659–2670.

Hauske, P., Ottmann, C., Meltzer, M., Ehrmann, M., and Kaiser, M. (2008). Allosteric Regulation of Proteases. ChemBioChem *9*, 2920–2928.

Kim, D.Y., and Kim, K.K. (2005). Structure and function of HtrA family proteins, the key players in protein quality control. J. Biochem. Mol. Biol. *38*, 266–274.

Liu, Y., Patricelli, M.P., and Cravatt, B.F. (1999). Activity-based protein profiling: the serine hydrolases. Proc. Natl. Acad. Sci. USA *96*, 14694–14699.

Mohamedmohaideen, N.N., Palaninathan, S.K., Morin, P.M., Williams, B.J., Braunstein, M., Tichy, S.E., Locker, J., Russell, D.H., Jacobs, W.R., Jr., and Sacchettini, J.C. (2008). Structure and function of the virulence-associated high-temperature requirement A of *Mycobacterium tuberculosis*. Biochemistry *47*, 6092–6102.

Monod, J., Wyman, J., and Changeux, J.P. (1965). On the Nature of Allosteric Transitions: A Plausible Model. J. Mol. Biol. *12*, 88–118.

Rhodius, V.A., Suh, W.C., Nonaka, G., West, J., and Gross, C.A. (2006). Conserved and variable functions of the sigmaE stress response in related genomes. PLoS Biol. *4*, e2.

Sohn, J., and Sauer, R.T. (2009). OMP peptides modulate the activity of DegS protease by differential binding to active and inactive conformations. Mol. Cell *16*, 67–74.

Sohn, J., Grant, R.A., and Sauer, R.T. (2007). Allosteric activation of DegS, a stress sensor PDZ protease. Cell *131*, 572–583.

Storoni, L.C., McCoy, A.J., and Read, R.J. (2004). Likelihood-enhanced fast rotation functions. Acta Crystallogr. D Biol. Crystallogr. *60*, 432–438.

Vande Walle, L., Lamkanfi, M., and Vandenabeele, P. (2008). The mitochondrial serine protease HtrA2/Omi: an overview. Cell Death Differ. *15*, 453–460.

Walsh, N.P., Alba, B.M., Bose, B., Gross, C.A., and Sauer, R.T. (2003). OMP peptide signals initiate the envelope-stress response by activating DegS protease via relief of inhibition mediated by its PDZ domain. Cell *113*, 61–71.

Wilken, C., Kitzing, K., Kurzbauer, R., Ehrmann, M., and Clausen, T. (2004). Crystal structure of the DegS stress sensor: How a PDZ domain recognizes misfolded protein and activates a protease. Cell *117*, 483–494.

Zeth, K. (2004). Structural analysis of DegS, a stress sensor of the bacterial periplasm. FEBS Lett. *569*, 351–358.